

Synthesis and Photochromism of Naphthopyrans Bearing Naphthalimide Chromophore: Predominant Thermal Reversibility in Color-Fading and Fluorescence Switch

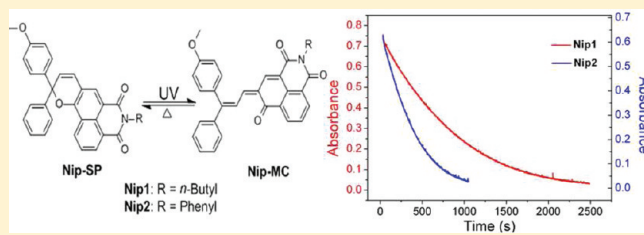
Liwen Song,[†] Yuheng Yang,[†] Qiong Zhang,^{†,‡} He Tian,[†] and Weihong Zhu^{*,†}

[†]Shanghai Key Laboratory of Functional Materials Chemistry, Key Laboratory for Advanced Materials and Institute of Fine Chemicals, East China University of Science and Technology, Shanghai 200237, P. R. China

[‡]Department of Theoretical Chemistry and Biology, Royal Institute of Technology, AlbaNova University Centre, 10691 Stockholm, Sweden

 Supporting Information

ABSTRACT: Two novel photochromic naphthopyrans containing naphthalimide moieties (**Nip1** and **Nip2**) were studied in solution under flash photolysis conditions, exhibiting highly photochromic response, rapid thermal bleaching rate and good fatigue-resistance. Owing to the different *N*-substituted imide groups at the naphthalimide units, the thermal bleaching rate of **Nip2** bearing phenyl on the naphthalimide unit is found to be approximately 2 times that of **Nip1** bearing *n*-butyl, indicating that the photochromic properties can be modulated with introduction of different functional groups on the naphthalimide unit. In **Nip1** and **Nip2**, the strong electron-withdrawing effect of the imide group incorporated at the naphthalimide moiety maintains several merits: (i) shifting absorption bands to longer wavelength, (ii) beneficial to an enhancement in the ratio of *transoid-cis* (TC) isomer and an increase in the transformation rate from *transoid-trans* (TT) to TC with respect to reference compound NP, and (iii) resulting in a preferable color bleaching rate and fading absolutely to their colorless state with thermal reversibility. As demonstrated in the system of NP, the slow transformation process from TT to TC might be the predominant dynamic step in thermal back process, leading to the residual color of NP being only faded to its original colorless state by visible light irradiation. The optical densities of colored forms for **Nip1** and **Nip2** are dependent upon the intensity of incident light, ensuring a possible application in the manufacture of ophthalmic lenses and smart windows. Moreover, the fluorescence of **Nip1** and **Nip2** can be switched on and off by photoinduced conversion between the closed and open forms.



INTRODUCTION

Photochromic materials have attracted much attention in recent years due to their potential application in ophthalmic lenses and molecular-level devices, such as molecular switches, optical data storage, logic gates, and molecule imaging.¹ Among various photochromic systems, naphthopyrans are known to exhibit excellent photochromic responses, good colorability, and rapid bleaching.² Generally, the photochromic naphthopyran system undergoes ring-opening with a color change via the photochemical cleavage of sp³ C—O bond, spontaneously reverting back to their original colorless closed form at dark or visible light irradiation when ceasing the UV luminous irradiation. To date, naphthopyans have become predominant in numerous naturally and biologically active compounds, and are explored in sensors,³ polymers,⁴ switches⁵ and organic gels.⁶ Because of the excellent photochromic response in a wide range of the visible spectrum from yellow to red and fast bleaching rate, the commercial application of naphthopyans in the manufacture of ophthalmic lenses and smart windows has attracted much interest for a decade, even has been applied in optical filters, diverse optical devices,

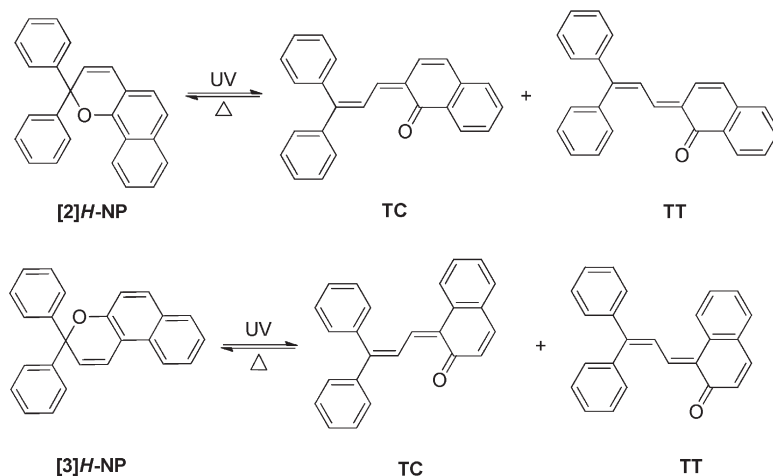
photographic apparatus, decorative objects, textiles, cosmetic products, and so on.⁷

For commercial application in ophthalmic lenses, it is necessary to keep photochromic molecules with highly efficient photo-response, large steady-state optical density, fast bleaching speed at ambient temperature, and excellent fatigue-resistance. Specifically, all the photochromic properties are critically dependent on their structural features with modifying different functional groups on naphthalene and/or two aromatic rings.⁸ For instance, various ring systems, such as fluorene⁹ and carbazole,¹⁰ fused to the naphthopyran moiety were synthesized for the sake of modulating their photochromic properties and commercial applications. With respect to 3,3-diaryl-3*H*-naphtho[2,1-*b*]pyrans ([3]*H*-NP, Scheme 1), photochromic 2,2-diaryl-2*H*-naphtho[1,2-*b*]pyrans ([2]*H*-NP) can promote the optical density of colored forms at ambient temperature and shift the absorption bathochromically to

Received: August 22, 2011

Revised: October 24, 2011

Published: October 25, 2011

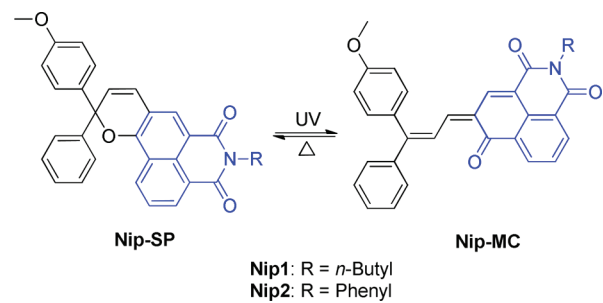
Scheme 1. Chemical Structures of [2]H-NP, [3]H-NP, and Open Forms TC and TT

neutral color range, which is quite suitable for commercial ophthalmic lenses. However, [2]H-NP always shows a distinct decrease in bleaching rate. What's even worse, the enhancement in photochromic response of [2]H-NP is invariably accompanied by an increase in the rate of photodegradation, resulting in the undesirable fatigue-resistance.²

1,8-naphthalimide and its derivatives with a strong electron-withdrawing imide group are a specific series of environmentally sensitive fluorophores, widely utilized in various fields due to their good chemical stability, large Stokes shift, and high fluorescent quantum yield.¹¹ More recently, we have incorporated naphthalimide units into photochromic spirooxazine and diarylethene systems,¹² especially realizing a significantly long lifetime in the open merocyanine (MC) forms. Bearing these considerations in mind, we designed and synthesized two novel naphthopyrans (**Nip1** and **Nip2** shown in Scheme 2) bearing a naphthalimide moiety with different *N*-substituted imide groups fused to the naphthalene moiety. Essentially, several merits with good photochromic properties are found in **Nip1** and **Nip2**: (i) their colored forms possess relatively large optical density and neutral color range, which intrinsically corresponds to the characteristics of 2*H*-naphtho[1,2-*b*]pyrans rather than that of 3*H*-naphtho[2,1-*b*]pyrans; (ii) the existence of naphthalimide unit with strong electron-withdrawing imide group can somehow eliminate the ratio of *transoid-trans* (TT) form, usually a slow step, or sharply increase the transformation rate from TT to *transoid-cis* (TC), thus facilitating the thermal back absolutely to closed form with a preferable color bleaching rate and thermal reversibility; and (iii) the fluorescence of naphthalimide unit can be switched on and off by photoinduced conversion. More specifically, the photochromic properties of **Nip1** and **Nip2** can be modulated with different *N*-substitution imide groups at the naphthalimide moiety, opening a new way to design molecular structures with various photochromic properties.

■ EXPERIMENTAL SECTION

Materials. 4-Bromo-1,8-naphthalic anhydride **1** (8.13 g, 29.4 mmol) and *n*-butylamine (6.45 g, 88.4 mmol) in acetic acid (90 mL) was refluxed under argon for 6 h. After cooling, the mixture was poured into water, resulting in yellow precipitate. It was filtered and recrystallized from acetic acid to afford 7.01 g of compound **2a** as a pale yellow crystal in 71.9% yield. ¹H-NMR (400 MHz, CDCl₃, ppm): δ 8.65 (d, *J* = 7.2 Hz, 1H, naphthalene-H), 8.56 (d, *J* = 8.0 Hz, 1H, naphthalene-H), 8.41 (d, *J* = 8.0 Hz, 1H, naphthalene-H), 8.03 (d, *J* = 7.6 Hz, 1H, naphthalene-H), 7.84 (t, *J* = 7.6 Hz, 1H, naphthalene-H), 4.17 (t, *J* = 7.6 Hz, 2H, -NCH₂-), 1.76–1.68 (m, 2H, -NCH₂CH₂-), 1.50–1.40 (m, 2H, -CH₂CH₃),

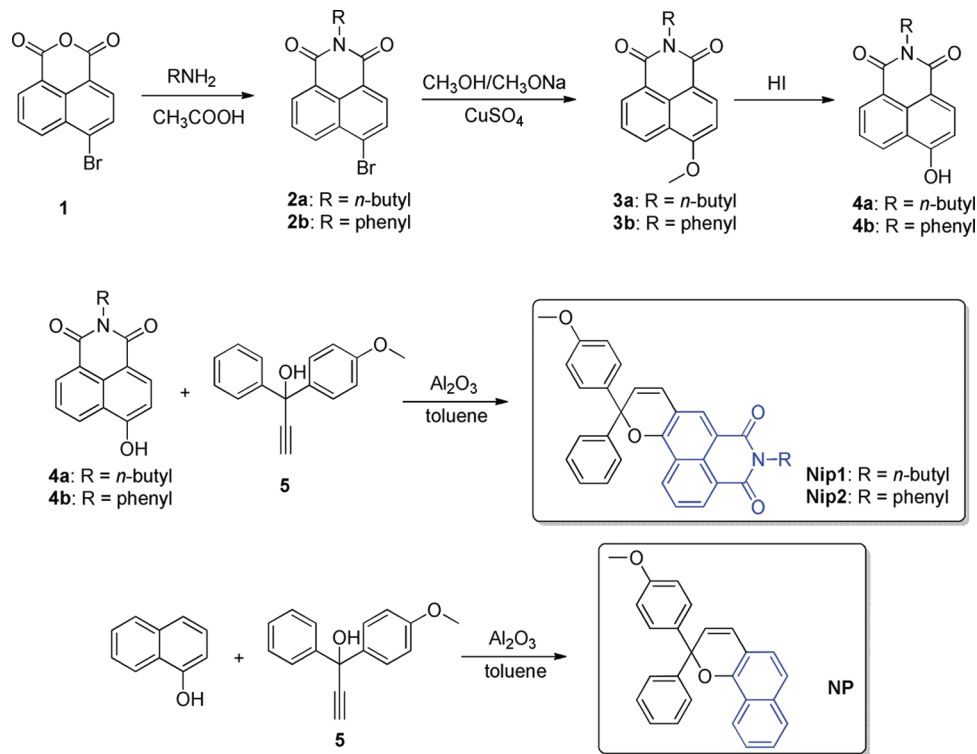
Scheme 2. Photochromic Reaction of Nip1 and Nip2

packages purchased from Qing-dao Haiyang Chemical Company, China.

Instrumentation. ¹H- and ¹³C-NMR spectra were recorded on Bruker AM-400 spectrometers with tetramethylsilane (TMS) as an internal reference and CDCl₃ or DMSO-*d*₆ as solvent. HRMS were recorded on a Waters LCT Premier XE spectrometer with methanol as solvent. Fluorescence spectra were recorded on a Horiba Fluoromax 4. Photochromic reaction was induced *in situ* by a continuous wavelength irradiation Hg/Xe lamp (Hamamatsu, LC6 Lightingcure, 200 W) equipped with narrow band interference filters of appropriate wavelengths (Semrock Hg01 for lirr = 365 nm, Semrock BrightLine FF01-575/25-25 for lirr = 575 nm). The irradiation power was measured using a photodiode from Ophir (PD300-UV). Absorption changes were monitored by a charge-coupled device (CCD) camera mounted on a spectrometer (Princeton Instruments).

Synthesis of 4-Bromo-*N*-butyl-1,8-naphthalimide (2a). A mixture of 4-bromo-1,8-naphthalic anhydride **1** (8.13 g, 29.4 mmol) and *n*-butylamine (6.45 g, 88.4 mmol) in acetic acid (90 mL) was refluxed under argon for 6 h. After cooling, the mixture was poured into water, resulting in yellow precipitate. It was filtered and recrystallized from acetic acid to afford 7.01 g of compound **2a** as a pale yellow crystal in 71.9% yield. ¹H-NMR (400 MHz, CDCl₃, ppm): δ 8.65 (d, *J* = 7.2 Hz, 1H, naphthalene-H), 8.56 (d, *J* = 8.0 Hz, 1H, naphthalene-H), 8.41 (d, *J* = 8.0 Hz, 1H, naphthalene-H), 8.03 (d, *J* = 7.6 Hz, 1H, naphthalene-H), 7.84 (t, *J* = 7.6 Hz, 1H, naphthalene-H), 4.17 (t, *J* = 7.6 Hz, 2H, -NCH₂-), 1.76–1.68 (m, 2H, -NCH₂CH₂-), 1.50–1.40 (m, 2H, -CH₂CH₃),

Scheme 3. Synthetic Routes of Nip1, Nip2, and Reference Compound NP



0.98 (*t*, *J* = 7.4 Hz, 3H, $-\text{CH}_2\text{CH}_3$). ^{13}C -NMR (100 MHz, CDCl_3 , ppm): δ 163.52, 133.11, 131.94, 131.13, 131.03, 130.51, 130.12, 128.88, 128.03, 123.08, 122.22, 40.38, 30.16, 20.38, 13.86. HRMS-ESI (*m/z*): [M + H]⁺ Calcd. for ($\text{C}_{16}\text{H}_{14}\text{BrNO}_2$), 332.0286, found: 332.0285.

Synthesis of 4-Bromo-N-phenyl-1,8-naphthalimide (2b).

A mixture of 4-bromo-1,8-naphthalic anhydride **1** (7.20 g, 26.0 mmol) and freshly distilled aniline (24.0 g, 0.26 mol) in acetic acid (100 mL) was refluxed under argon for 24 h. After cooling, the mixture was poured into water, resulting in yellow precipitate. It was filtered and recrystallized from acetic acid to afford 7.60 g of compound **2b** as a pale yellow crystal in 83.0% yield. ¹H-NMR (400 MHz, CDCl₃, ppm): δ 8.70 (d, *J* = 7.2 Hz, 1H, naphthalene-H), 8.64 (d, *J* = 8.5 Hz, 1H, naphthalene-H), 8.46 (d, *J* = 8.0 Hz, 1H, naphthalene-H), 8.08 (d, *J* = 7.6 Hz, 1H, naphthalene-H), 7.89 (t, *J* = 7.2 Hz, 1H, naphthalene-H), 7.58–7.56 (m, 2H, phenyl-H), 7.51–7.48 (m, 1H, phenyl-H), 7.31 (d, *J* = 7.2 Hz, 2H, phenyl-H). ¹³C-NMR (100 MHz, CDCl₃, ppm): δ 163.77, 163.73, 135.10, 133.61, 132.44, 131.58, 131.22, 130.74, 130.67, 129.47, 129.31, 128.88, 128.57, 128.21, 123.21, 122.33. HRMS-ESI (*m/z*): [M + H]⁺ Calcd. for (C₁₈H₁₀BrNO₂), 351.9973, found: 351.9977.

Synthesis of 4-Methoxy-N-butyl-1,8-naphthalimide (3a).

4-Bromo-N-butyl-1,8-naphthalimide **2a** (6.01 g, 18.1 mmol), sodium methoxide (7.76 g, 0.14 mol) and copper sulfate (0.66 g, 2.8 mmol) were mixed in dry methanol (80 mL). The reaction mixture was refluxed under argon for 8 h. After cooling, the resulting mixture was filtered to give pale yellow solid as a crude product. Then the solid was washed with 10% (v/v) hydrochloric acid (30 mL × 3) and water (20 mL × 3) to afford 4.47 g of compound **3a** as a pale green needle-shaped crystal in 87.3% yield. ¹H-NMR (400 MHz, CDCl₃, ppm): δ 8.57 (d, *J* = 7.2 Hz, 1H, naphthalene—H), 8.52 (d, *J* = 8.0 Hz, 2H, naphthalene—H),

7.68 (t, J = 7.6 Hz, 1H, naphthalene-H), 7.01 (d, J = 8.4 Hz, 1H, naphthalene-H), 4.16 (t, J = 7.6 Hz, 2H, -NCH₂-), 4.12 (s, 3H, -OCH₃), 1.75-1.68 (m, 2H, -NCH₂CH₂-), 1.50-1.40 (m, 2H, -CH₂CH₃), 0.98 (t, J = 7.3 Hz, 3H, -CH₂CH₃). ¹³C-NMR (100 MHz, CDCl₃, ppm): δ 164.45, 163.88, 160.66, 133.30, 131.40, 129.23, 128.47, 125.85, 123.36, 122.36, 115.06, 105.10, 56.16, 40.07, 30.26, 20.42, 13.89. HRMS-ESI (*m/z*): [M + H]⁺ Calcd. for (C₁₇H₁₇NO₃), 284.1287, found: 284.1283.

Synthesis of 4-Methoxy-N-phenyl-1,8-naphthalimide (3b).

4-Bromo-N-phenyl-1,8-naphthalimide **2b** (7.50 g, 21.3 mmol), sodium methoxide (9.20 g, 0.17 mmol) and copper sulfate (0.66 g, 2.8 mmol) were mixed in dry methanol (100 mL). The reaction mixture was refluxed under argon for 15 h. After cooling, the resulting mixture was filtered to give yellow-green solid as a crude product. Then the solid was washed with 10% (v/v) hydrochloric acid (100 mL × 3) and water (100 mL × 3) to afford 6.10 g of compound **3b** as a pale yellow solid in 94.0% yield. ¹H-NMR (400 MHz, CDCl₃, ppm): δ 8.65–8.59 (m, 3H, naphthalene–H), 7.73 (d, J = 7.6 Hz, 1H, naphthalene–H), 7.58–7.53 (m, 2H, naphthalene–H), 7.48–7.45 (m, 1H, naphthalene–H), 7.31 (d, J = 7.6 Hz, 2H, naphthalene–H), 7.08 (d, J = 8.0 Hz, 1H, phenyl–H), 4.16 (s, 3H, –OCH₃). ¹³C-NMR (100 MHz, CDCl₃, ppm): δ 164.69, 164.10, 161.09, 135.71, 133.87, 131.94, 129.79, 128.99, 128.73, 128.55, 126.04, 123.67, 122.56, 115.15, 105.32, 56.30. HRMS-ESI (*m/z*): [M + H]⁺ Calcd. for (C₁₉H₁₃NO₃), 304.0974, found: 304.0971.

Synthesis of 4-Hydroxy-N-butyl-1,8-naphthalimide (4a).

A mixture of 4-methoxy-*N*-butyl-1,8-naphthalimide **3a** (2.08 g, 7.3 mmol) and 57% (v/v) hydroiodic acid (100 mL) was refluxed under argon for 10 h. After cooling, the resulting mixture was filtered, then the crude product was washed with water (50 mL × 3) to afford yellow-green solid. The crude product was purified by column chromatography on silica (petroleum ether:ethyl

acetate = 3:1, v/v) to afford 1.16 g of compound **4a** as a pale yellow solid in 59.0% yield. ¹H-NMR (400 MHz, DMSO-*d*₆, ppm): δ 8.53 (dd, *J* = 8.4 Hz, *J*₂ = 1.2 Hz, 1H, naphthalene-H), 8.47 (dd, *J*₁ = 7.2 Hz, *J*₂ = 1.2 Hz, 1H, naphthalene-H), 8.36 (d, *J* = 8.4 Hz, 1H, naphthalene-H), 7.76 (t, *J* = 7.2 Hz, 1H, naphthalene-H), 7.16 (d, *J* = 8.4 Hz, 1H, naphthalene-H), 4.02 (t, *J* = 7.4 Hz, 2H, -NCH₂-), 1.64–1.58 (m, 2H, -NCH₂CH₂-), 1.39–1.30 (m, 2H, -CH₂CH₃), 0.92 (t, *J* = 7.3 Hz, 3H, -CH₂CH₃). ¹³C-NMR (100 MHz, DMSO-*d*₆, ppm): δ 163.59, 162.92, 160.17, 133.45, 131.02, 129.09, 128.78, 125.49, 122.31, 121.74, 112.55, 109.89, 40.12, 29.70, 19.78, 13.68. HRMS-ESI (*m/z*): [M – H]⁺ Calcd. for (C₁₆H₁₅NO₃), 268.0974, found: 268.0978.

Synthesis of 4-Hydroxy-*N*-phenyl-1,8-naphthalimide (4b). A mixture of 4-methoxy-*N*-phenyl-1,8-naphthalimide **3b** (1.50 g, 4.90 mmol) and 57% (v/v) hydroiodic acid (60 mL) was refluxed under argon for 15 h. After cooling, the resulting mixture was filtered, then the crude product was washed with water (50 mL × 3) to afford 0.90 g of yellow-green solid. The product was directly used without further purification for the next step.

Synthesis of 5-Butyl-10-(4-methoxyphenyl)-10-phenylbenzo-[*de*]pyrano[2,3-*g*]isoquinoline-4,6(5H,10H)-dione (Nip1). In a 50 mL three-necked flask, equipped with a Dean–Stark apparatus, 4-hydroxy-*N*-butyl-1,8-naphthalimide **4a** (700 mg, 2.6 mmol), propargyl alcohol derivative **5** (834 mg, 3.5 mmol), and aluminum oxide (7.00 g) were mixed in toluene (25 mL). The reaction mixture was refluxed under argon for 5 h. After cooling, the resulting mixture was filtered, and the filter cake was washed with dichloromethane (50 mL × 3). Then the filtrate and the scrubbing solution were combined. After concentration, the compound was purified by column chromatography on silica (petroleum ether:dichloromethane = 5:1, v/v) to give crude product, then recrystallized from ethanol to afford 360 mg of compound **Nip1** as a pale yellow solid in 28.3% yield. ¹H-NMR (CDCl₃, 400 MHz, ppm): δ 8.61 (dd, *J*₁ = 8.4 Hz, *J*₂ = 1.2 Hz, 1H, naphthalene-H), 8.56 (dd, *J*₁ = 7.2 Hz, *J*₂ = 1.2 Hz, 1H, naphthalene-H), 8.33 (s, 1H, naphthalene-H), 7.71 (t, *J* = 7.6 Hz, 1H, naphthalene-H), 7.49–7.47 (m, 2H, phenyl-H), 7.41–7.35 (m, 4H, phenyl-H), 7.34–7.32 (m, 1H, phenyl-H), 6.89–6.84 (m, 3H, =CH, phenyl-H), 6.27 (d, *J* = 10.0 Hz, 1H, =CH), 4.17 (t, *J* = 7.6 Hz, 2H, -NCH₂-), 3.79 (s, 3H, -OCH₃), 1.74–1.66 (m, 2H, -CH₂CH₂-), 1.47–1.41 (m, 2H, -CH₂CH₂-), 0.98 (t, *J* = 7.2 Hz, 3H, -CH₂CH₃). ¹³C-NMR (100 MHz, CDCl₃, ppm): δ 164.37, 163.84, 159.36, 153.63, 144.28, 136.06, 131.48, 130.67, 129.49, 128.75, 128.44, 128.39, 128.32, 127.93, 126.71, 126.25, 122.71, 122.51, 116.62, 115.25, 113.72, 84.98, 55.27, 40.08, 30.25, 20.38, 13.86. HRMS-ESI (*m/z*): [M + H]⁺ Calcd. for (C₃₂H₂₇NO₄), 490.2018, found: 490.2018.

Synthesis of 10-(4-Methoxyphenyl)-5,10-diphenylbenzo-[*de*]pyrano[2,3-*g*]isoquinoline-4,6(5H,10H)-dione (Nip2). In a 50 mL three-necked flask, equipped with a Dean–Stark apparatus, 4-hydroxy-*N*-phenyl-1,8-naphthalimide **4b** (400 mg, 1.38 mmol), propargyl alcohol derivative **5** (438 mg, 1.84 mmol) and aluminum oxide (4.00 g) were mixed in toluene (20 mL). The reaction mixture was refluxed under argon for 7 h. After cooling, the resulting mixture was filtered, and the filter cake was washed with dichloromethane (50 mL × 3). Then the filtrate and the scrubbing solution were combined. After concentration, the compound was purified by column chromatography on silica (petroleum ether:dichloromethane = 1:2, v/v) to give crude product, then recrystallized from ethanol to afford 140 mg of compound **Nip2** as a pale yellow solid in 20.0% yield. ¹H-NMR (400 MHz, CDCl₃, ppm): δ 8.65 (d, *J* = 8.0 Hz, 1H, naphthalene-H), 8.58 (d, *J* = 7.2 Hz, 1H,

naphthalene-H), 8.35 (s, 1H, naphthalene-H), 7.72 (t, *J* = 8.0 Hz, 1H, naphthalene-H), 7.55–7.51 (m, 2H, phenyl-H), 7.48–7.44 (m, 3H, phenyl-H), 7.41–7.35 (m, 4H, phenyl-H), 7.32–7.27 (m, 3H, phenyl-H), 6.88–6.84 (m, 3H, =CH, phenyl-H), 6.27 (d, *J* = 10.0 Hz, 1H, =CH), 3.78 (s, 3H, -OCH₃). ¹³C-NMR (100 MHz, CDCl₃, ppm): δ 164.56, 163.99, 159.40, 154.01, 144.23, 136.00, 135.63, 131.95, 131.06, 129.91, 129.35, 128.91, 128.78, 128.70, 128.59, 128.49, 128.44, 128.00, 126.73, 126.38, 122.91, 122.77, 122.46, 116.78, 115.21, 113.76, 85.13, 55.30. HRMS-ESI (*m/z*): [M + H]⁺ Calcd. for (C₃₄H₂₃NO₄), 510.1705, found: 510.1713.

Synthesis of 2-(4-Methoxyphenyl)-2-phenyl-2*H*-benzo-[*h*]chromene (NP). In a 50 mL three-necked flask, equipped with a Dean–Stark apparatus, naphthalen-1-ol (1.0 g, 6.9 mmol), propargyl alcohol derivative **5** (2.2 g, 9.2 mmol) and aluminum oxide (10.0 g) were mixed in toluene (40 mL). The reaction mixture was refluxed under argon for 9 h. After cooling, the resulting mixture was filtered, and the filter cake was washed with dichloromethane (100 mL × 3). Then the filtrate and the scrubbing solution were combined. After concentration, the compound was purified by column chromatography on silica (petroleum ether:dichloromethane = 5:1, v/v) to afford 210 mg of pale yellow solid in 8.4% yield. ¹H-NMR (400 MHz, DMSO-*d*₆, ppm): δ 8.29 (d, *J* = 8.4 Hz, 1H, phenyl-H), 7.82 (d, *J* = 8.0 Hz, 1H, phenyl-H), 7.57–7.48 (m, 4H, phenyl-H), 7.44–7.41 (m, 3H, phenyl-H), 7.34 (t, *J* = 7.6 Hz, 2H, phenyl-H), 7.30–7.23 (m, 2H, phenyl-H), 6.90–6.84 (m, 3H, phenyl-H, =CH), 6.49 (d, *J* = 10.0 Hz, 1H, =CH), 3.69 (s, 3H, -CH₃). ¹³C-NMR (100 MHz, DMSO-*d*₆, ppm): δ 163.75, 152.06, 150.40, 142.04, 139.31, 133.46, 133.37, 132.99, 132.77, 132.53, 131.71, 131.27, 131.17, 129.83, 129.19, 128.64, 126.51, 125.74, 120.98, 118.82, 87.44, 60.26. HRMS-ESI (*m/z*): [M + H]⁺ Calcd. for (C₂₆H₂₀O₂), 365.1542, found: 365.1537.

■ RESULTS AND DISCUSSION

Synthesis. Naphthopyrans always play a great role in the manufacture of ophthalmic lenses. Generally, this important application requires that photochromic compounds possess several specific characteristics: (i) large optical density and neutral color range, that is, the absorption spectra in the colored form almost cover the whole visible spectrum, (ii) fast photoresponse, and (iii) rapid color fading rate. However, these preconditions cannot concur in traditional 2*H*-naphtho[1,2-*b*]pyrans, which always possess relatively large optical density and neutral color range, but unfavorable fading rate synchronously. Evans et al. reported a general method for realizing fast and synchronizing photochromic switching for photochromic dyes including naphthopyrans.^{4c,d} To further develop the photochromic properties of naphthopyran derivatives, a naphthalimide unit with different *N*-substituted imide groups was incorporated. As illustrated in Scheme 3, the target compounds **Nip1** and **Nip2** were synthesized by Claisen rearrangement of propargyl-aryl ethers prepared from 4-hydroxy-1,8-naphthalimide (**4**), which was synthesized from the raw material of 4-bromo-1,8-naphthalic anhydride (**1**) via three steps (imidation, Williamson ether condensation, and Zeisel ether cleavage). The reference compound NP was directly prepared by *α*-naphthol and propargyl alcohol derivative **5**. Notably, using excess acidic Al₂O₃ as a catalyst,¹³ the synthesis in the Claisen rearrangement of propargyl-aryl ethers could become straightforward with an easy purification and preferable yield. Their chemical structures were well confirmed by ¹H-NMR, ¹³C-NMR, and HRMS. The character ¹H-NMR

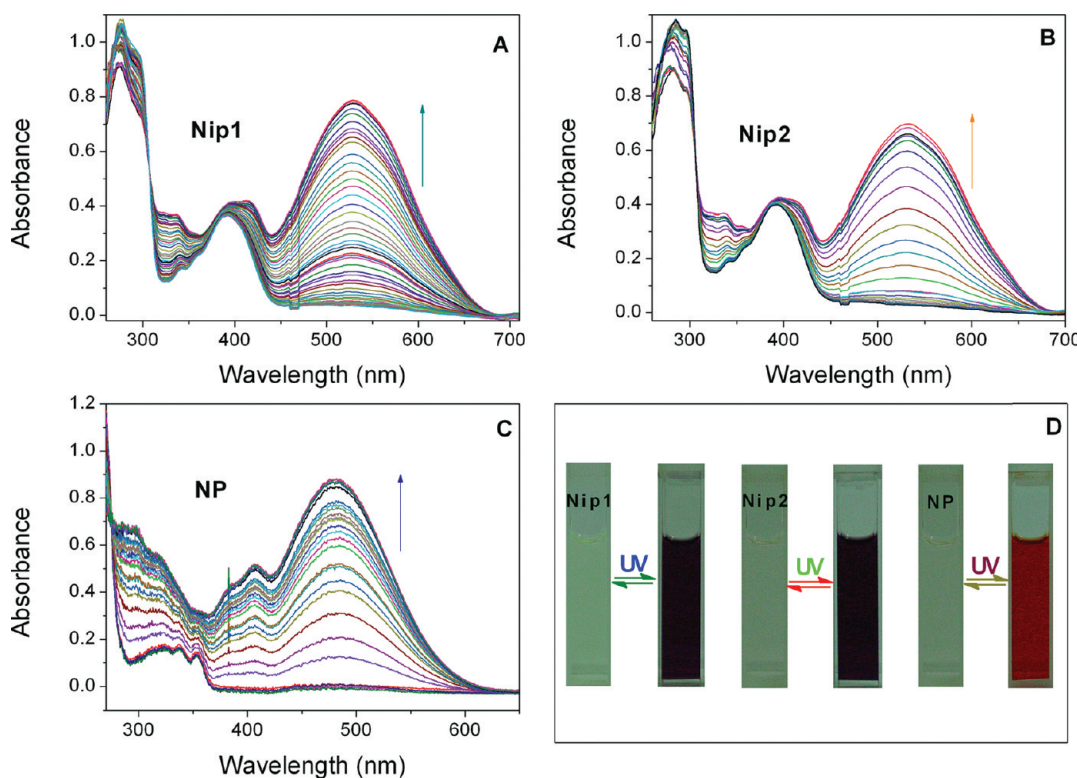


Figure 1. Absorption spectral changes upon UV irradiation at 365 nm in acetonitrile (5.0×10^{-5} M) at 293 K: (A) Nip1, (B) Nip2, (C) NP, and (D) photographic images of Nip1, Nip2, and NP in acetonitrile before and after UV irradiation.

resonance for the vinyl proton adjacent to the carbon bearing the heteroatom (O) can be found as doublets as 6.27 ppm for Nip1 and Nip2 and 6.49 ppm for NP with a characteristic coupling constant (J) of 10.0 Hz. Here the specific proton resonance of Nip1 and Nip2 shifts upfield by 0.22 ppm. In ^{13}C -NMR, the sp^3 -hybridized carbon is also characteristic, appearing at 84.98, 85.13, and 87.44 ppm for Nip1, Nip2, and NP, respectively (see the Experimental Section and Supporting Information for details).

Photochromic Properties. The evaluation of photochromic behaviors for Nip1, Nip2, and NP involves the knowledge of some relevant parameters, related to the spectra of closed and open forms, kinetic thermal back rate, and fatigue resistance. All photochromic properties of Nip1 and Nip2 induced by photo-irradiation were measured in acetonitrile solution under flash photolysis at 293 K. As shown in Figure 1, the absorption spectra of Nip1 and Nip2 do not show substantial differences. Before UV light irradiation, two absorption peaks are observed at 280 and 385 nm. Compared with the conventional naphthopyran NP, the absorption band at 385 nm for Nip1 and Nip2 results from the incorporated naphthalimide moiety (Figure 1).¹¹ Upon irradiation with UV light (365 nm), a new visible absorption band centered at 530 nm becomes emerged, while the original peak at 280 nm is decreased to some extent, indicative of the formation of the open MC form (Scheme 2). It is resulted from the photochemical cleavage of the sp^3 C–O bond that leads to the planarization of the two originally orthogonal cycles, giving rise to an increase in the extent of π conjugation in the MC structure. Consequently, the colorless solution turns purple, resulting from the open form (Figure 1D). Under the same condition, the reference compound NP shows similar photochromic properties. What is different, under 365 nm UV light irradiation, is that the new visible absorption band is centered at 480 nm (Figure 1C),

Table 1. Absorption Data of Nip1, Nip2, and NP before and after UV Irradiation in Acetonitrile (5.0×10^{-5} M)

compounds	SP form (λ_{\max} , nm)	MC form (λ_{\max} , nm)
Nip1	280, 385	280, 425, 530
Nip2	280, 385	280, 425, 530
NP	320	410, 480

which is blue-shifted by 50 nm with respect to Nip1 and Nip2. This can be attributed to the naphthalimide unit incorporated at the naphthopyran fragment, thus giving a strong electron-withdrawing effect to favor the red-shifted absorption in MC form. The optical properties of Nip1, Nip2, and NP before and after irradiation were summarized in Table 1.

Notably, compared with NP, the red-shifted characteristics in the absorption band of Nip1 and Nip2 are quite suitable for the application in ophthalmic lenses.^{13a} As illustrated in Figure 1, their absorption spectra in the colored form almost cover the whole visible spectrum. Moreover, upon 365 nm light irradiation, the absorption spectra between 300 and 400 nm are also increased. It is known that the wave band of UV light can cause skin aging and graveness damaging. Hence, the generic nature of Nip1 and Nip2 is beneficial to the application in eye-protective glasses since the harmful UV light can be effectively absorbed.

Thermochromism Properties. It is known that the photo-coloration of 2H-naphtho[1,2-*b*]pyran ([2]H-NP) under UV light irradiation can induce the formation of two open forms TT and TC; while TC isomer rapidly returns to the uncolored closed form, the TT isomer is thermally more stable (Scheme 1).¹⁴ The colored form of Nip1 and Nip2 can be thermally back to their closed form (CF) when the photoirradiation is ceased

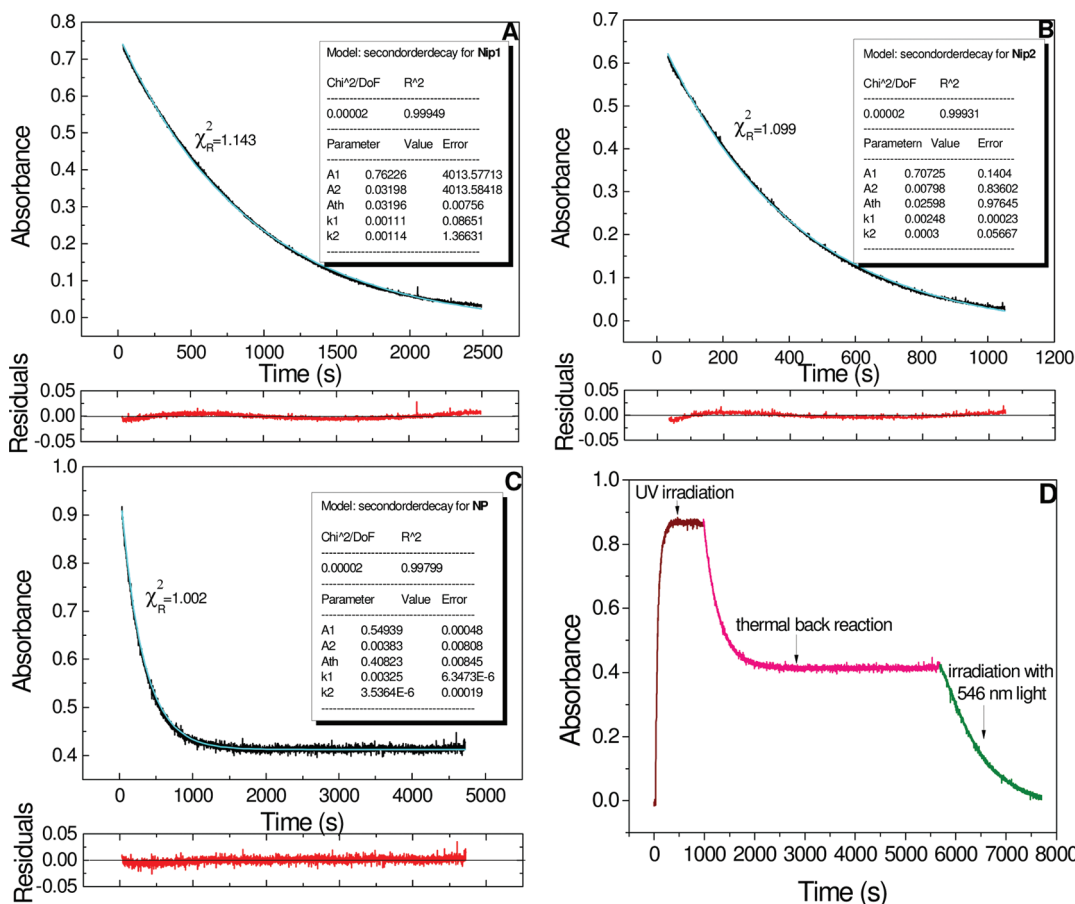


Figure 2. The biexponential (second order) decay model and experimental thermal fading kinetics in acetonitrile (5.0×10^{-5} M) at 293 K: (A) Nip1, (B) Nip2, (C) NP (black line: data measured; cyan line: the second order decay model fitted; red line: the absorbance residuals at testing time). Inset: the second order decay model parameters. The monitored wavelength was at 530, 530, and 480 nm for Nip1, Nip2 and NP, respectively. (D) Reverse reaction of reference compound NP (5.0×10^{-5} M) monitored at 480 nm in acetonitrile at 293 K.

Table 2. Spectrokinetic Data of Thermal Bleaching for Nip1, Nip2, and NP (5.0×10^{-5} M in Acetonitrile) at 293 K^a

compounds	λ_{max} (nm)	$\tau_{1/2}$ (s)	$\tau_{3/4}$ (s)	k_1 (10^{-3} s $^{-1}$)	k_2 (10^{-3} s $^{-1}$)	A_0	A_1	A_2	A_{th}
Nip1	530	620	1200	1.11	1.14	0.757	0.762	0.032	0.032
Nip2	530	298	540	2.48	0.30	0.626	0.707	0.080	0.026
NP	480	760		3.25	0.0035	0.917	0.549	0.004	0.408

^a k_1 , k_2 , A_1 , and A_2 are the fitting parameters from eq 1; λ_{max} , $\tau_{1/2}$, $\tau_{3/4}$, A_0 , and A_{th} were obtained from experimental data.

(Figure 2A,B). Two steps proceed in the color-faded course, that is, from TC to CF form, and from TT to TC form, then thermal back to colorless CF form. Notably, the process of TC to CF is usually rapid; the change from TT to CF is quite slow. The convenient measurement of decoloration rate can be described as $\tau_{1/2}$ and $\tau_{3/4}$ values, which are the time that it takes from the absorbance to reduce by 1/2 and 3/4 of the initial absorbance in the colored form, respectively.¹⁵ The bleaching kinetics, determined from the absorption-time data sets, can be fitted well to the biexponential decay (eq 1).^{4c}

$$A(\tau) = A_1 e^{-k_1 \tau} + A_2 e^{-k_2 \tau} + A_{\text{th}} \quad (1)$$

where $A(\tau)$ is the absorbance at λ_{max} of Nip1 and Nip2; A_1 and A_2 are the contributions to the initial absorbance A_0 ; k_1 and k_2 are exponential decay rate constants of fast and slow components,

respectively; and A_{th} is the residual coloration (offset) at the termination of testing time. As depicted in Figure S1 in the Supporting Information, it was found that the fading times $\tau_{1/2}$ and $\tau_{3/4}$ for Nip2 are 298 and 540 s, respectively, which are quite smaller than that of Nip1 ($\tau_{1/2} = 620$ s, $\tau_{3/4} = 1200$ s). From eq 1, the fading rate constants (Figure 2B) can be obtained for Nip2 ($k_1 = 2.48 \times 10^{-3}$ s $^{-1}$, $k_2 = 3.0 \times 10^{-4}$ s $^{-1}$), while the corresponding data for Nip1 (Figure 2A) is 1.11×10^{-3} and 1.14×10^{-3} s $^{-1}$, respectively. Obviously, the fast rate constants (k_1) of the spontaneous thermal bleaching course for Nip1 and Nip2 (Table 2) are 1.11×10^{-3} and 2.48×10^{-3} s $^{-1}$, respectively, indicating that the *N*-substituted imide group at naphthalimide unit has an effect on the thermal bleaching rate to some extent. As illustrated in Figure 3, the purple appearance of Nip2 in acetonitrile was gradually bleached in about 20 min, while Nip1 still maintained its purple color. It is found that the thermal bleaching

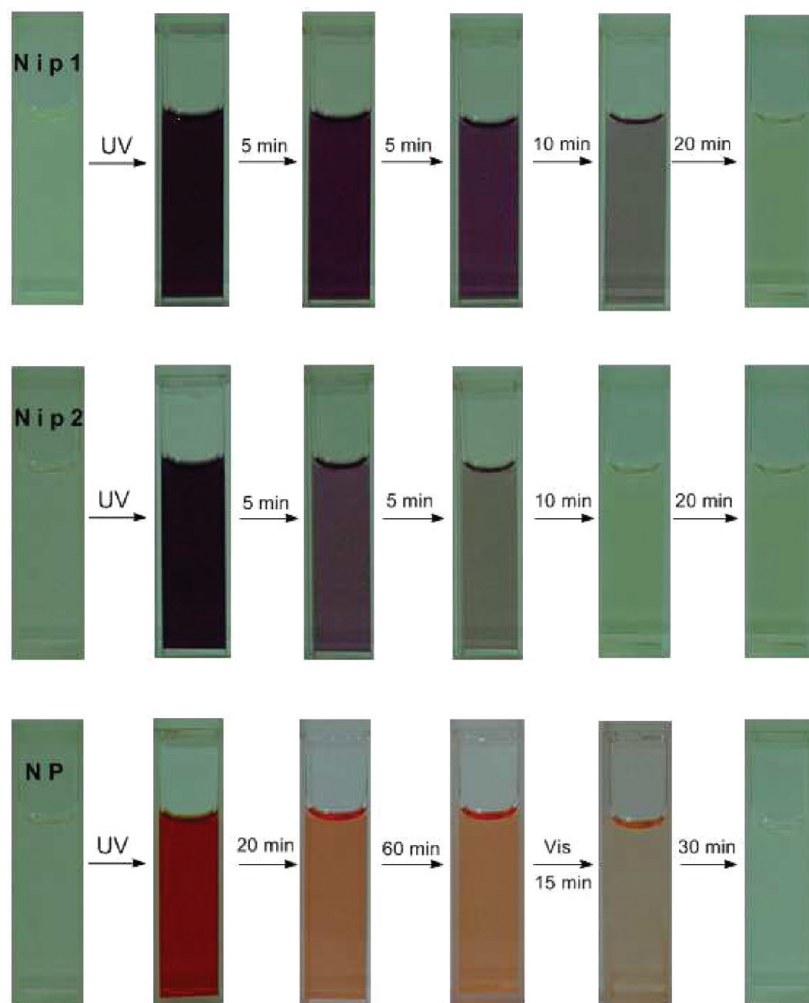


Figure 3. Photographic images of Nip1, Nip2, and NP in acetonitrile (5.0×10^{-5} M) before and after UV irradiation, and their thermal bleaching in dark at 293 K.

rate of Nip2 in solution under dark is faster than that of Nip1, which can be attributed to the different *N*-substituted imide groups in naphthalimide unit. Also the spectrokinetic data determined for the photochromic naphthopyrans are summarized in Table 2. Notably, after thermal back reaction, the MC forms of Nip1 and Nip2 are almost transformed to the colorless closed forms, and even the color of their solution was not detectable by the naked eye.

As shown in Figure 2D, NP reached a photostationary state (PSS) upon UV light irradiation. When the UV irradiation was ceased, the colored form of NP commenced bleaching, and after about 1000 s, the optical density reduced to half of its original state value. Although the thermal back reaction time was maintained for an additional 4000 s, the optical density value still maintained stability. That is, the residual visible coloration cannot be spontaneously faded to the absolute colorless. However, upon 546 nm light irradiation, the residual color can be efficiently faded to its original colorless state. In order to fully understand the photochromic difference, the thermal fading reaction of NP was also investigated. As depicted in Figure 2C, the rate constants (*k*) of the spontaneous thermal bleaching course are 3.25×10^{-3} and $3.54 \times 10^{-6} \text{ s}^{-1}$, fitted with biexponential decay performed based on Levenberg–Marquardt (LM) iteration. Accordingly, as depicted in Figure 2D, the reverse reaction of reference compound NP can

successively undergo two courses through (i) thermal back reaction and (ii) visible light irradiation.

However, despite a larger decay rate constant in the case of reference compound NP (Table 2), its red appearance can still be maintained for another 1 h with no more color fading. This is because the residual color of NP is only faded to its original colorless state by visible light irradiation. As mentioned above, two steps proceed in the color-faded course, that is, from TC to CF form (usually rapid), and from TT to TC form, then thermal back to CF form (usually slow). This means that, for NP, the slow transformation process from TT to TC form might be the predominant dynamic step in the thermal back process. Therefore, we consider that, in the system of Nip1 and Nip2, the existence of the naphthalimide unit can somehow eliminate the ratio of TT form or sharply increase the transformation rate from TT to TC, thus facilitating the thermal back absolutely to CF form (Figure 2A,B). By contrast, the reference compound NP cannot bleach absolutely under the same condition (Figure 2C, D), which can be attributed to the more contribution from stable TT form under the same conditions, and must be irradiated by visible light to return to its original CF state. As found in Figure 2A,B, the residual absorption of Nip1 and Nip2 is very low, almost reaching zero. So we did not take the irradiation with

Table 3. The Optimized Geometries, Populations, and Relative Energies ΔE for TC and TT Isomers of Nip1, Nip2, and NP

Compounds	TC	TT
Nip1	Optimized Geometries	
	Populations (%) ΔE^a (kcal/mol)	35 0.36
Nip2	Optimized Geometries	
	Populations (%) ΔE^a (kcal/mol)	42 0.19
NP	Optimized Geometries	
	Populations (%) ΔE^a (kcal/mol)	16 0.98
Nip1	Optimized Geometries	
	Populations (%) ΔE^a (kcal/mol)	65 0
Nip2	Optimized Geometries	
	Populations (%) ΔE^a (kcal/mol)	58 0
NP	Optimized Geometries	
	Populations (%) ΔE^a (kcal/mol)	84 0

^a The relative energy of TC isomer with respect to TT isomer.

visible light to the very low residual absorption of **Nip1** and **Nip2**. When ceasing UV light irradiation, we can use visible light to bleach the color form of **Nip1** and **Nip2**.

Computational Study of Nip1, Nip2, and NP. To gain insight into the electron-withdrawing effect of the imide group and different *N*-substitution incorporated at the naphthalimide moiety, we carried out quantum chemical calculations on **Nip1**, **Nip2**, and the reference compound **NP** with the Gaussian 09 program.¹⁶ The geometries were optimized with the hybrid B3LYP exchange-correlation functional and 6-31G(d,p) basis set. On the basis of the optimized structures, more accurate energies were achieved by single-point calculations with the larger basis set 6-311+G(d,p). Frequency calculations were performed at the B3LYP/6-31G(d,p) level of theory to obtain zero-point energies (ZPEs) and to confirm the nature of the stationary points. The solvent effect was taken into account within the polarizable continuum model with acetonitrile as solvent.

The calculation results are summarized in Table 3. As calculated for both **Nip1** and **Nip2**, the TT isomer is more stable than the TC isomer. The TT isomer is calculated to be more favorable than the TC isomer by 0.36 and 0.19 kcal mol⁻¹ for **Nip1** and **Nip2**, respectively, while for **NP**, this value is 0.98 kcal mol⁻¹. The populations for the TC and TT isomers are deduced from the relative energies according to the Boltzmann distribution. The populations of TC isomers are 35% and 42% for **Nip1** and **Nip2**, respectively. That is, in the MC forms, the portions of TC isomer for **Nip1** and **Nip2** are almost 2.18–2.63 times that for the reference compound **NP**, which just takes 16% portions. Apparently, owing to the larger population of thermally unstable TC isomer and smaller energy difference between TC and TT isomers, the thermal bleaching rate of **Nip2** is faster than **Nip1**,

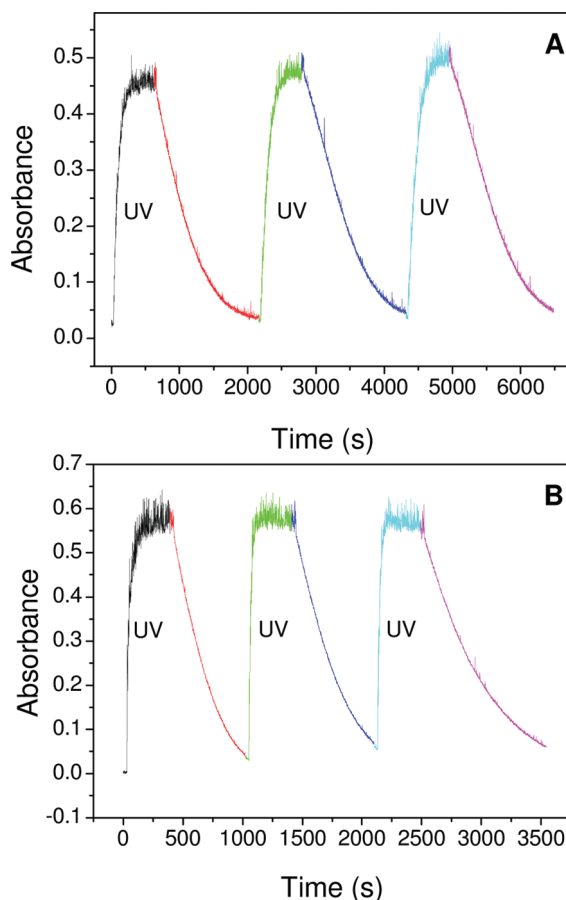


Figure 4. Time-dependent photocaloration of **Nip1** (A) and **Nip2** (B) in acetonitrile (2.19×10^{-4} M) at 293 K by UV irradiation at 365 nm, and the subsequent thermal fading when the irradiation was ceased. The monitored wavelength was at 530 nm.

and is much faster than that of the reference compound **NP**, an observation in exact consistence with the observed experiment results in the thermal bleaching decay. Obviously, in **Nip1** and **Nip2** the strong electron-withdrawing effect of the imide group incorporated at naphthalimide moiety are preferable to an enhancement in the ratio of TC isomer and an increase in the transformation rate from TT to TC with respect to reference compound **NP**, thus resulting in a preferable color bleaching rate and fading absolutely to their colorless state, behaving as classical thermo-reversible photochromic photochromes. In addition, another reason accounting for the slower bleaching rate of **Nip1** than **Nip2** might be the energy loss via the thermal vibration of the long linear alkyl chain on *N*-substitution incorporated at the naphthalimide moiety in **Nip1**.

Photocaloration/Thermal Bleaching Cycles. The photocaloration investigation revealed that both **Nip1** and **Nip2** can undergo coloration in several seconds with UV light irradiation. As depicted in Figure 4, it takes only about 40 s for the optical density of **Nip2** to reach half of the value at its PSS, and about 100 s to PSS, these values are smaller than those of the reference compound **NP**, which need almost 400 s to reach PSS under the same measurement conditions. Obviously, the developed naphthopyrans **Nip1** and **Nip2** possess highly photoresponse, an important precondition to application in ophthalmic plastic lenses. In addition, fatigue resistance is another important factor to evaluate material applications. A preliminary investigation of fatigue resistance for

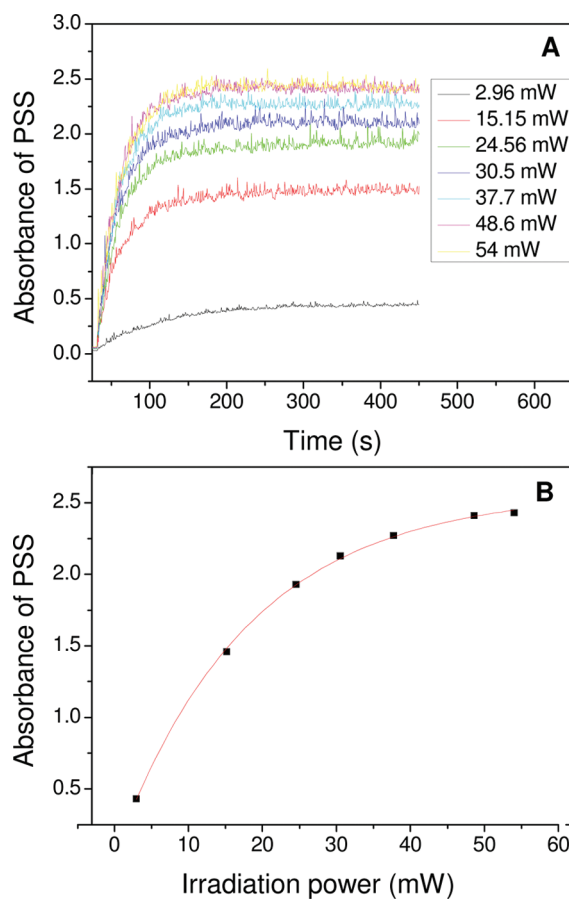


Figure 5. (A) Absorption changes of **Nip1** in acetonitrile (5.0×10^{-5} M) at PSS upon photoirradiation power. (B) The absorbance at PSS of **Nip1** increases as a function of photoirradiation power.

naphthopyran derivatives **Nip1** and **Nip2** was performed, apparently revealing a quite good reproducibility (Figure 4). However, after each decoloration process, a residual visible absorbance remained, even though the color of solution was not detectable by the naked eye. By contrast, the optical density at PSS after successive coloration and decolorization cycles was not altered. Consequently, the low residual absorption might not result from the photodegradation. In other investigated naphthopyrans, the residual absorption resulted from the TT isomer of the open form, and could disappear by irradiation with visible light. This is explained by assuming that the TT isomeric photoproduct is thermally stable but photoreversible, and needs to be under visible light to revert to the original colorless form.^{13,17}

Irradiation-Dependent Optical Density. Furthermore, the optical density at PSS is closely related to the irradiation power. As illustrated in Figure 5, the optical density of **Nip1** at PSS was quite small when the input power was 2.96 mW. Under this condition, sufficient color change cannot be detected. However, with more powerful incident light, the optical density increased sharply, and the value tended to be a real stationary state until about 50 mW, then the color change of **Nip1** in acetonitrile before and after photoirradiation was very distinct. As known, naphthopyrans are T-type photochromic dyes, which exhibit a considerable competition between forward and backward reaction. When ceasing UV light irradiation at ambient temperature, the thermal back reaction is rather fast when the photoirradiation power is not intense enough,

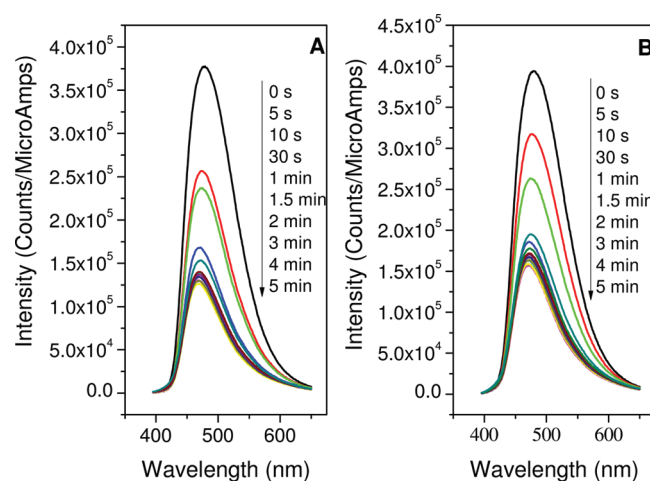


Figure 6. Fluorescence changes in acetonitrile (5.0×10^{-5} M) upon 365 nm irradiation at 293 K: (A) **Nip1**, (B) **Nip2**. The obtained fluorescence was excited at 390 nm.

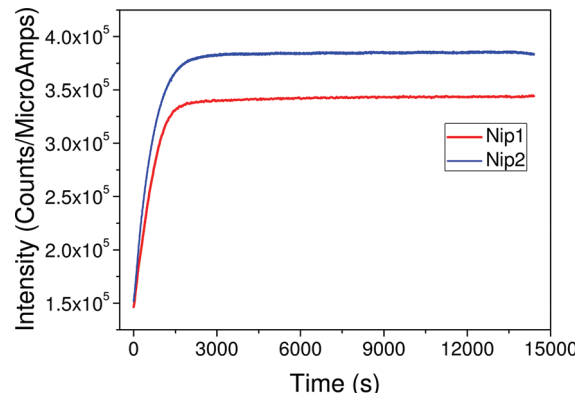


Figure 7. Fluorescence enhancement of **Nip1** and **Nip2** during dark decoloration at 293 K in acetonitrile (5.0×10^{-5} M). The monitored wavelength was at 480 nm.

and the reverse reaction has a tendency toward backward thermal bleaching. When the irradiation lamp is powerful enough so that the equilibrium constant of the forward reaction is larger than that of the backward reaction, the total reaction is inclined to be coloration. As a consequence, the more powerful the incident light, the more intense the absorbance, and the more distinct the color change that can be detected. Bearing this feature in mind, both **Nip1** and **Nip2** are suitable for industrial application in smart windows. When sunlight is intense at noon, the intense ultraviolet radiation of sunlight can be effectively absorbed, thus realizing the modulation of the indoor beam and temperature according to the intensity of sunlight.

Fluorescence Switch. It is known that 1,8-naphthalimides are highly fluorescent moieties with good chemical stability.¹¹ Interestingly, the fluorescence of the naphthalimide moiety in **Nip1** and **Nip2** can be switched on and off by photoinduced conversion between the closed and open forms. That is, the closed form of **Nip1** and **Nip2** shows the characteristic fluorescence from the naphthalimide moiety at 480 nm, which diminishes quickly under the UV light irradiation. During the dark decoloration, the fluorescence of the solution can be recovered. As depicted in Figure 6, upon irradiation with a UV light of 365 nm, the fluorescence intensity

of **Nip1** and **Nip2** reduced quickly in a few seconds. Upon irradiation for 5 min, the fluorescence reached a stable state, and the intensity ($\lambda_{\text{ex}} = 390 \text{ nm}$, $\lambda_{\text{em}} = 480 \text{ nm}$) reduced by 68% and 62% for **Nip1** and **Nip2**, respectively. Here the fluorescence quenching of the naphthalimide moiety in the open form of **Nip1** and **Nip2** may result from the electronic delocalization throughout the MC form (Scheme 2). Again, the fluorescence intensity can be increased at dark when ceasing the UV light irradiation (Figure 7). The process of fluorescence on and off can be repeated between the closed and open forms, suggestive of potential application in recording media and other optic apparatuses.

CONCLUSIONS

Two new photochromic naphthopyrans **Nip1** and **Nip2** bearing naphthalimide units have been synthesized and investigated. Both two compounds can reversibly change color under UV light and the removal of irradiation. The incorporation of a naphthalimide unit into the classical naphthopyran structure enables longer wavelength absorption bands. Remarkably, the electron-withdrawing imide group of the naphthalimide unit incorporated at naphthopyrans results in the open MC forms, exhibiting a significantly fast thermal bleaching rate. Because of the larger population of thermally unstable TC isomers and the low energy difference between TC and TT isomers, the thermal bleaching rate of **Nip2** bearing phenyl on the naphthalimide unit is faster than **Nip1** bearing *n*-butyl, much faster than that of reference compound **NP**. The thermal fading reversibility of **Nip1** and **Nip2** is substantially complete, while the reference compound **NP** exhibits thermal and photochemical reversibility in color-fading. As demonstrated in the system of **NP**, the slow transformation process from TT to TC might be the predominant dynamic step in the thermal back process, leading to the residual color of **NP** being only faded to its original colorless state by visible light irradiation. The fluorescence of **Nip1** and **Nip2** can be switched on and off by photoinduced conversion between the closed and open forms. Moreover, their optical densities of colored forms are dependent upon the intensity of photoinduced sources, ensuring a possible application in the manufacture of ophthalmic lenses and smart windows.

ASSOCIATED CONTENT

Supporting Information. ¹H-NMR, ¹³C-NMR, and HRMS spectra of **Nip1**, **Nip2**, **NP**, and other intermediates, thermal back reaction of **Nip1** and **Nip2** at dark after 365 nm UV light irradiation, and reverse reaction of **NP** upon 546 nm light irradiation. This information is available free of charge via the Internet at <http://pubs.acs.org>.

AUTHOR INFORMATION

Corresponding Author

*Fax: (+86) 21-6425-2758. E-mail: whzhu@ecust.edu.cn

ACKNOWLEDGMENT

This work was financially supported by NSFC/China, the Oriental Scholarship, SRFDP 200802510011, and the Fundamental Research Funds for the Central Universities (WK1013002).

REFERENCES

- (1) (a) Irie, M. *Chem. Rev.* **2000**, *100*, 1685–1716. (b) Tian, H.; Yang, S. *J. Chem. Soc. Rev.* **2004**, *33*, 85–97. (c) Samachetty, H. D.; Branda, N. R. *Pure Appl. Chem.* **2006**, *78*, 2351–2359. (d) Yuan, W. F.; Sun, L.; Tang, H. H.; Wen, Y. Q.; Jiang, G. Y.; Huang, W. H.; Jiang, L.; Song, Y. L.; Tian, H.; Zhu, D. B. *Adv. Mater.* **2005**, *17*, 156–160. (e) Guo, K. P.; Chen, Y. *J. Mater. Chem.* **2009**, *19*, 5790–5793. (f) Remón, P.; Hammarskjöld, M.; Li, S. M.; Kahnt, A.; Pischel, U.; Andréasson, J. *Chem.—Eur. J.* **2011**, *17*, 6492–6500. (g) Tian, Z. Y.; Wu, W. W.; Li, A. D. Q. *ChemPhysChem* **2009**, *10*, 2577–2591. (h) Zou, Y.; Yi, T.; Xiao, S. Z.; Li, F. Y.; Li, C. Y.; Gao, X.; Wu, J. C.; Yu, M. X.; Huang, C. H. *J. Am. Chem. Soc.* **2008**, *130*, 15750–15751. (i) Wang, S.; Qi, Q.; Li, C.; Ding, G.; Kim, S.-H. *Dyes Pigm.* **2011**, *89*, 188–192.
- (2) (a) Lokshin, V.; Sama, A.; Metelitsa, A. V. *Russ. Chem. Rev.* **2002**, *71*, 893–916. (b) di Nunzio, M. R.; Gentili, P. L.; Romani, A.; Favaro, G. *ChemPhysChem* **2008**, *9*, 768–775. (c) Crano, J. C.; Flood, T.; Knowles, D.; Kumar, A.; Gemert, B. V. *Pure Appl. Chem.* **1996**, *68*, 1395–1398.
- (3) (a) Kumar, S.; Hernandez, D.; Hoa, B.; Lee, Y.; Yang, J. S.; McCurdy, A. *Org. Lett.* **2008**, *10*, 3761–3764. (b) Glebov, E. M.; Smolentsev, A. B.; Korolev, V. V.; Plyusnin, V. F.; Chebunkova, A. V.; Paramonov, S. V.; Fedorova, O. A.; Lokshin, V.; Samat, A. *J. Phys. Org. Chem.* **2009**, *22*, 537–545. (c) Ahmed, S. A.; Tanaka, M.; Ando, H.; Iwamoto, H.; Kimura, K. *Eur. J. Org. Chem.* **2003**, 2437–2442. (d) Tan, W. J.; Zhou, J.; Li, F. Y.; Yi, T.; Tian, H. *Chem.—Asian J.* **2011**, *6*, 1263–1268. (e) Piao, X. J.; Zou, Y.; Wu, J. C.; Li, C. Y.; Yi, T. *Org. Lett.* **2009**, *11*, 3818–3821.
- (4) (a) Kahle, I.; Tröber, O.; Treutsch, S.; Richter, H.; Grünler, B.; Hemeltjen, S.; Schlesinger, M.; Mehring, M.; Stefan, S. *J. Mater. Chem.* **2011**, *21*, 5083–5088. (b) Ercole, F.; Malic, N.; Harrisson, S.; Davis, T. P.; Evans, R. A. *Macromolecules* **2010**, *43*, 249–261. (c) Malic, N.; Campbell, J. A.; Ali, A. S.; York, M.; D’Souza, A.; Evans, R. A. *Macromolecules* **2010**, *43*, 8488–8501. (d) Evans, R. A.; Hanley, T. L.; Skidmore, M. A.; Davis, T. P.; Such, G. K.; Yee, L. H.; Ball, G. E.; Lewis, D. A. *Nat. Mater.* **2005**, *4*, 249–253.
- (5) (a) Guo, K. P.; Chen, Y. *J. Phys. Org. Chem.* **2010**, *23*, 207–210. (b) Gabbott, C. D.; Heron, B. M.; Kilner, C.; Kolla, S. B. *Chem. Commun.* **2010**, *46*, 8481–8483. (c) Ahmed, S. A.; Tanaka, M.; Ando, H.; Iwamoto, H.; Kimura, K. *Tetrahedron* **2004**, *60*, 3211–3220. (d) Yassar, A.; Rebière-Galy, N.; Frigoli, M.; Moustrou, C.; Samat, A.; Guglielmetti, R.; Jaafari, A. *Synth. Met.* **2001**, *124*, 23–27.
- (6) (a) Pardo, R.; Zayat, M.; Levy, D. C. R. *Chimie* **2010**, *13*, 212–226. (b) Katritzky, A. R.; Sakhuja, R.; Khelashvili, L.; Shanab, K. *J. Org. Chem.* **2009**, *74*, 3062–3065. (c) Coelho, P. J.; Carvalho, L. M.; Goncalves, L. F. F. F.; Silva, C. J. R.; Campos, A. M.; Gomes, M. J. *J. Sol-Gel Sci. Technol.* **2010**, *56*, 203–211.
- (7) (a) Little, A. F.; Christie, R. M. *Color. Technol.* **2010**, *126*, 164–170. (b) Corns, S. N.; Partington, S. M.; Towns, A. D. *Color. Technol.* **2009**, *125*, 249–261.
- (8) (a) Shilova, E. A.; Pépe, G.; Samat, A.; Moustrou, C. *Tetrahedron* **2008**, *64*, 9977–9982. (b) Sallenave, X.; Delbaere, S.; Vermeersch, G.; Pozzo, J. L. *J. Phys. Org. Chem.* **2007**, *20*, 872–877. (c) Arnall-Culliford, J. C.; Terai, Y.; Sgarabotto, P.; Campredon, M.; Giusti, G. *J. Photochem. Photobiol. A: Chem.* **2003**, *159*, 7–16.
- (9) (a) Coelho, P. J.; Salvador, M. A.; Oliveira, M. M.; Carvalho, L. M. *J. Photochem. Photobiol. A: Chem.* **2005**, *172*, 300–307. (b) Ortica, F.; Romani, A.; Blackburn, F.; Favaro, G. *Photochem. Photobiol. Sci.* **2002**, *1*, 803–808.
- (10) Oliveira, M. M.; Salvador, M. A.; Delbaere, S.; Berthet, J.; Vermeersch, G.; Micheau, J. C.; Coelho, P. J.; Carvalho, L. M. *J. Photochem. Photobiol. A: Chem.* **2008**, *198*, 242–249.
- (11) (a) Gan, J. A.; Tian, H.; Wang, Z. H.; Chen, K. C.; Hill, J.; Lane, P. A.; Rahn, M. D.; Fox, A. M.; Bradley, D. D. C. *J. Organomet. Chem.* **2002**, *645*, 168–175. (b) Qian, X. H.; Xiao, Y.; Xu, Y. F.; Guo, X. F.; Qian, J. H.; Zhu, W. P. *Chem. Commun.* **2010**, *46*, 6418–6436. (c) Sun, Y.; Wei, S.; Yin, C.; Liu, L. S.; Hu, C. M.; Zhao, Y. Y.; Ye, Y. X.; Hu, X. Y.; Fan, J. *Bioorg. Med. Chem. Lett.* **2011**, *21*, 3798–3804. (d) Georgiev, N. I.; Bojinov, V. B.; Nikolov, P. S. *Dyes Pigm.* **2009**, *81*, 18–26. (e) Bojinov, V. B.; Georgiev, N. I.; Marinova, N. V. *Sens. Actuators, B: Chem.* **2010**, *148*, 6–16.
- (12) (a) Meng, X. L.; Zhu, W. H.; Guo, Z. Q.; Wang, J. Q.; Tian, H. *Tetrahedron* **2006**, *62*, 9840–9845. (b) Meng, X. L.; Zhu, W. H.;

Zhang, Q.; Feng, Y. L.; Tan, W. J.; Tian, H. *J. Phys. Chem. B* **2008**, *112*, 15636–15645.

(13) (a) Queiroz, M.; Abreu, A. S.; Ferreira, P. M. T.; Oliveira, M. M.; Dubest, R.; Aubard, J.; Samat, A. *Org. Lett.* **2005**, *7*, 4811–4814. (b) Gabbott, C. D.; Heron, B. M.; Kolla, S. B.; Kilner, C.; Coles, S. J.; Horton, P. N.; Hursthouse, M. B. *Org. Biomol. Chem.* **2008**, *6*, 3096–3104.

(14) (a) Delbaere, S.; Micheau, J. C.; Vermeersch, G. *J. Org. Chem.* **2003**, *68*, 8968–8973. (b) Sriprom, W.; Neto, C.; Perrier, S. *Soft Matter* **2010**, *6*, 909–914. (c) Ercole, F.; Malic, N.; Davis, T. P.; Evans, R. A. *J. Mater. Chem.* **2009**, *19*, 5612–5623.

(15) (a) Guo, K. P.; Chen, Y. *J. Mater. Chem.* **2010**, *20*, 4193–4197. (b) Han, S. L.; Chen, Y. *J. Mater. Chem.* **2011**, *21*, 4961–4965.

(16) Frisch, M. J.; Trucks, G. W.; Schlegel, H. B.; Scuseria, G. E.; Robb, M. A.; Cheeseman, J. R.; Scalmani, G.; Barone, V.; Mennucci, B.; Petersson, G. A.; et al. *Gaussian 09*, revision A.02; Gaussian, Inc.: Wallingford CT, 2009.

(17) Ortica, F.; Romani, A.; Blackburn, F.; Favaro, G. *Photochem. Photobiol. Sci.* **2002**, *1*, 803–808.